Experimental studies of the NaRb ground-state potential up to the $v''=76$ level

O. Docenko, O. Nikolayeva, M. Tamanis, and R. Ferber
Department of Physics, University of Latvia, 19 Rainis Boulevard, Riga LV-1586, Latvia

E. A. Pazyuk and A. V. Stolyarov
Department of Chemistry, Moscow State University, Moscow 119899, Russia

(Received 13 June 2002; published 22 November 2002)

Laser induced fluorescence spectra of the $C\,^1\Sigma^+ - X\,^1\Sigma^+$ system of $^{23}Na^{85}Rb$ and $^{23}Na^{87}Rb$ have allowed vibrational levels of the electronic ground state up to $v''=76$, spanning 99.85% of the potential well to be observed. The ground-state term values have been fitted to a Dunham polynomial expansion, and also to a direct modified Lennard-Jones (MLJ) potential. The analytical MLJ construction allowed us to match previous measured term values for $v''\leqslant 30$ with long-range behavior of the potential through the intermediate internuclear distance region covered by the present investigation.

DOI: 10.1103/PhysRevA.66.052508 PACS number(s): 33.15.Mt, 33.20.−t

I. INTRODUCTION

In last decades alkali diatomics have proved to be a focus of intensive experimental studies and *ab initio* calculations of adiabatic potential curves for both excited and ground electronic states. Special attention has been put on the determination of highly accurate ground-state potential in a wide internuclear separation range and, in particular, on the opportunity of including larger internuclear distances into consideration to adequately model the photoassociation spectroscopy of cold atoms [1] and other laser cooling experiments. Moreover, the accurate ground-state potential is necessary to refine the excited-state potentials constructed by the ''difference-based'' method [2,3].

The ground-state potential of the NaK dimer was studied systematically by the Fourier-transform laser induced fluorescence (FT LIF) spectroscopy of the $C^1\Sigma^+ \rightarrow X^1\Sigma^+$ transition [4]. The obtained high accuracy term values up to near dissociation limit were analyzed from the perspective of their long-range behavior to construct the hybrid $X^1\Sigma^+$ state potential [5]. For the KRb molecule Dunham molecular constants have been recently determined [6] from the $A^1\Sigma^+ \rightarrow X^1\Sigma^+$ fluorescence for the first 88 vibrational levels of the $X^1\Sigma^+$ state, and the relevant $X^1\Sigma^+$ potential has been constructed up to internuclear distance of 10.4 Å (99.3% of the potential well depth). The LIF spectra of the $B^1\Pi \rightarrow X^1\Sigma^+$ system, recorded by the FT interferometer, have been recently applied to observe the first 47 vibrational levels of the $^{39}K^7Li$ ground state [7]. The obtained term values were reduced to Dunham molecular constants [8] as well as directly to a numerical inverted perturbation approach (IPA) potential curve [9]. The FT LIF $A^1\Sigma_u^+ \rightarrow X^1\Sigma_g^+$ spectra were used to measure the term values of all three Rb_2 isotopomers, which allowed involving ground-state levels up to $v''=113$, covering 99.8% of the ground-state potential well [10]. The isotope-substituted data set was applied to a Dunham-type analysis as well as to a direct fit to the analytical ''modified Lennard-Jones'' (MLJ) potential curve [11].

As distinct from the above species, direct experimental information on the ground state of the NaRb molecule is still rather limited. Indeed, highly accurate term values of the $X^1\Sigma^+$ state obtained [12] by the Doppler-free laser polarization spectroscopy of the $B^1\Pi - X^1\Sigma^+$ transition, are available for the vibrational levels $v''\in[0,30]$ which cover only 57% of the well depth. Moreover, only for the two lowest vibrational levels $v''=0,1$, the term values were measured [13] in a wide range of rotational quantum numbers $J''\in[0,80]$ while those for $v''\in[2,6]$ and $v''\in[5,30]$ were limited by $J''\in[1,42]$ [13] and $J''=10,12$ [12], respectively. A rather accurate value of the dissociation energy $D_e=5030.75\pm 0.10$ cm^{-1} for the $X^1\Sigma^+$ state has been recently determined [14] based on (i) the improved Rydberg-Klein-Rees (RKR) curve for the $a^3\Sigma^+$ state $U_a^{RKR}(R)$; (ii) the long-range Coulomb energy contribution $\Delta U_C(R)=-C_6/R^6-C_8/R^8-C_{10}/R^{10}$, with dispersion coefficients C_6, C_8, and C_{10} calculated in Ref. [15]; (iii) the exchange potential $\Delta U_E(R)$ approximated by the Smirnov-Chibisov [16] asymptotic form $\Delta U_E(R)=-CR^\alpha e^{-\beta R}$, where parameter C was obtained from a difference *ab initio* $X^1\Sigma^+$ and $a^3\Sigma^+$ potential [17], i.e., $\Delta U_E^{ab}(R)=1/2[U_X^{ab}(R)-U_a^{ab}(R)]$. Then, the complete hybrid potential-energy curve for the $X^1\Sigma^+$ ground state was constructed [14] by using (i) the RKR curve for $v''\in[0,30]$ from Ref. [12]; (ii) the long-range potential $U_X^{LR}(R)=D_e+\Delta U_C(R)+\Delta U_E(R)$; (iii) the difference-based potential for the attractive wall of the curve corresponding to intermediate internuclear distance, i.e., $U_X^{att}(R)=U_a^{RKR}(R)+2\Delta U_E^{ab}(R)$; (iv) the repulsive wall extrapolated above the $v''=30$ level of the RKR potential by an exponential $U_X^{rep}(R)=Ae^{-bR}$. The absolute accuracy of the derived hybrid potential in the $v''>30$ region is apparently limited by the accuracy of $U_X^{att}(R)$ and $U_X^{rep}(R)$ functions since their error is expected to increase as R decreases. Therefore, the authors of Ref. [14] have concluded that further experimental studies for higher $v''>30$ values are required to refine the NaRb $X^1\Sigma^+$-state potential curve in the intermediate energy region.

The usual way of extending the range of ground-state vibrational levels v'' observed in emission for alkali dimers is to use, instead of the $B-X$, either the $A-X$ or $C-X$ system. In the present study we made use of the opportunity to excite the high vibrational levels of the $C^1\Sigma^+$ electronic

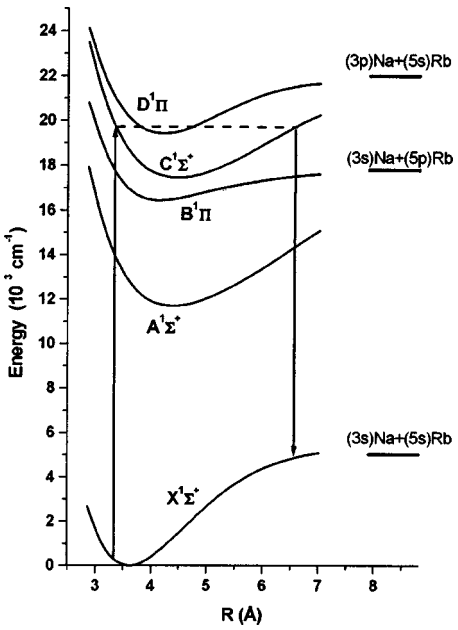

FIG. 1. Potential-energy curves [2] for the low-lying singlet states of NaRb and LIF excitation and observation scheme.

state in a direct $C^1\Sigma^+ \leftarrow X^1\Sigma^+$ transition and to exploit the subsequent visible emission. As follows from the *ab initio* potential curves [2] depicted in Fig. 1, there is enough reason to predict that $C^1\Sigma^+ \rightarrow X^1\Sigma^+$ fluorescence can be excited by visible Ar^+-laser lines and it should stretch up to sufficiently high v'' levels of the $X^1\Sigma^+$ state due to considerable shifting between the respective potentials (similarly the case of the NaK molecules, see Ref. [4]). In the early paper on the NaRb LIF studies [18] it was reported that the Ar^+-laser 514.5-nm line induced fluorescence spectrum was observed up to 14 000 cm^{-1} (710 nm). This spectrum was later [13] recognized as the transitions ending on high v'' levels of the $X^1\Sigma^+$ state. The simplicity of the excitation scheme and the convenient visible range of LIF encouraged us to undertake further investigations of the $C \rightarrow X$ emission in order to reach as many as possible $v'' > 30$ rovibronic levels and, thus, to fill the gap between the accurate low v'' experimental data [12,13] and calculated long-range data [14]. To consistently process different sets of experimental and theoretical data, we have adopted as the most appropriate direct potential fit analysis based on the MLJ potential, which has been recently developed [11] and successfully exploited for an extremely accurate Rb_2 ground-state potential study [10].

The paper is structured as follows. Section II describes experimental details aimed in obtaining transition frequencies, as well as raw data processing yielding the NaRb ground-state term values $T^{expt}_{v''J''}$ covering vibrational levels up to $v''=76$, or 99.85% of the potential well depth. Section III contains a description of a conventional Dunham-type analysis of the above $T^{expt}_{v''J''}$ values, as well as of their direct fit to MLJ potential followed by concluding remarks in Sec. IV.

II. EXPERIMENT

A. Experimental details

NaRb molecules were formed from a 4:1 mixture of natural Rb (containing 72% of ^{85}Rb and 28% of ^{87}Rb) and Na metals in an alkali-resistant glass thermal cell at the temperature ca. 550 K. LIF was excited by an Ar^+-laser (Spectra Physics 171) operating in a single-mode regime at 514.5 nm wavelength. LIF has been dispersed at right angles by a double monochromator with 1200 lines/mm gratings and 5 Å /mm inverse dispersion in first diffraction order, providing at reasonable slits 0.2-Å spectral resolution. Fluorescence progressions have been detected up to 680 nm by a FEU-79 photomultiplier operating in a photon counting regime. Simultaneously detected Ar and Ne discharge lines have been used as frequency standards. The average inaccuracy of the LIF line positions was estimated as ca. 0.1 cm^{-1}.

B. Analysis of the $C^1\Sigma^+ \rightarrow X^1\Sigma^+$ progressions

As is well established [2,18], the 514.5-nm Ar^+-laser line excites $D^1\Pi \leftarrow X^1\Sigma^+$ transition in the NaRb molecule (P, Q, and R transitions ending on $v' \in [0,6]$ have been identified), followed by intensive $D^1\Pi \rightarrow X^1\Sigma^+$ LIF terminating at ca. 580 nm and covering $v'' \in [0,34]$ region [2]. However it is possible to observe under the same excitation rather intensive LIF progressions, see Fig. 2, not connected with the D

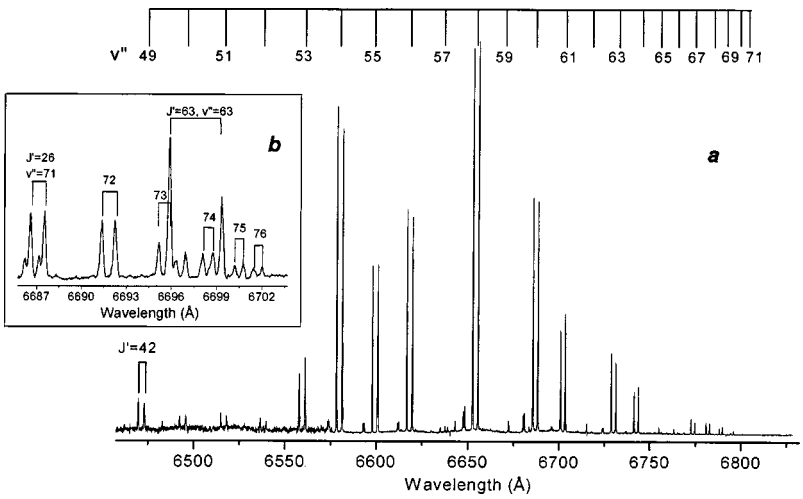

FIG. 2. Pieces of the $C \rightarrow X$ fluorescence spectrum induced by absorption of the Ar^+-laser 514.5 nm line. (a) $C^1\Sigma^+(v',J'=42) \leftarrow X^1\Sigma^+(v''=1,J''=43)$ in $^{23}Na^{85}Rb$; (b) $C^1\Sigma^+(v',J'=26) \leftarrow X^1\Sigma^+(v''=4,J''=25)$ in $^{23}Na^{85}Rb$ and $C^1\Sigma^+(v',J'=63) \leftarrow X^1\Sigma^+(v''=1,J''=62)$ in $^{23}Na^{87}Rb$.

TABLE I. $C^1\Sigma^+(v',J')-X^1\Sigma^+(v'',J'')$ transitions induced by the 514.5 nm (19 429.826 cm^{-1}) Ar^+-laser line. $T^{expt}_{v'J'}=T^{calc}_{v''J''}+\nu_{laser}$ are the respective $C^1\Sigma^+$ term values. Parameters $\Delta T_{v'J'}=T^{expt}_{v'J'}-T^{shift}_{v'J'}$ account for an uncertainty in the fluorescence series origin, $T^{shift}_{v'J'}$ denoting the corrected term value. $\Delta T^{Dunh}_{v'J'}$ and $\Delta T^{MLJ}_{v'J'}$ values were obtained within the Dunham type and direct MLJ potential fits, respectively. The numbers in parentheses are equal to two standard deviations. All energies are in cm^{-1}.

Isotopomer	v''	J''	J'	$T^{expt}_{v'J'}$	v'' range	$\Delta T^{Dunh}_{v'J'}$	$\Delta T^{MLJ}_{v'J'}$
$^{23}Na^{85}Rb$	1	12	13	19600.11	[21,70]	0.12(±0.04)	0.10(±0.05)
$^{23}Na^{85}Rb$	4	25	26	19947.63	[26,76]	−0.01(±0.04)	−0.01(±0.02)
$^{23}Na^{85}Rb$	1	43	42	19720.75	[15,71]	0.19(±0.09)	0.21(±0.11)
$^{23}Na^{87}Rb$	3	61	60	20056.69	[27,71]	0.48(±0.25)	0.35(±0.22)
$^{23}Na^{87}Rb$	1	62	63	19858.11	[24,71]	0.37(±0.30)	0.18(±0.16)

$-X$ system [2]. These progressions, possessing maximum intensity in the red spectral range, can be attributed to the $C-X$ system originating from high $v'>30$ levels. Such assumption is proved by tentative evaluation of the respective Franck-Condon factors using the difference-based *ab initio* $C^1\Sigma^+$ potential [2]. Experimental justification is as follows. First, no singlet red LIF progressions have been observed, only the doublet-type series which correspond to the $\Sigma-\Sigma$ transitions. Additionally, we have undertaken a Stark-effect-based test which showed that applying an external electric field up to 5000 V/cm did not cause any changes in the red LIF spectra. If it were the $D^1\Pi$ state, due to the Stark-induced e/f mixing in the $^1\Pi$ state, see Refs. [2,19], the triplet LIF spectra would be observed instead of the doublet spectra. The above considerations allowed us to conclude that LIF progressions observed in the red spectral range up to 680 nm originated from the $C^1\Sigma^+$ state.

Figure 2 presents fragments of the $C^1\Sigma^+\rightarrow X^1\Sigma^+$ fluorescence progressions in the range of high ground-state v'' values. To assign the transitions in this spectrum, it was necessary to go to smaller $v''<30$ region where accurate spectroscopic constants of the $^{23}Na^{85}Rb$ ground state from Refs. [13,14] are applicable. This was the most difficult part of the experiment due to smaller intensities of the $C-X$ transitions in the low v'' region and the partial overlapping with $D-X$ transitions. As a result, we have registered and assigned five $C^1\Sigma^+\rightarrow X^1\Sigma^+$ fluorescence progressions presented in Table I which were excited by different modes of the 514.5 nm line. For small J ($J<27$) the progressions assignment was based on Dunham molecular constants [14], while for large J, as well as for the $^{23}Na^{87}Rb$ isotopomer, a numerical solution of the radial Schrödinger equation was exploited with the RKR potential constructed by molecular constants from Ref. [14].

The measured $C^1\Sigma^+(v';J')\rightarrow X^1\Sigma^+(v'';J'')$ progression wave numbers ν^{expt}_{C-X} have been transformed into the corresponding term values of the ground state as $T^{expt}_{v''J''}=T^{expt}_{v'J'}-\nu^{expt}_{C-X}$. Term values of the upper $C^1\Sigma^+$ state $T^{expt}_{v'J'}$ (where v' values remained unknown) have been obtained by adding the laser frequency ν_{laser} to the energy of the initial absorbing ground state, leading to $T^{expt}_{v'J'}=T^{calc}_{v''J''}+\nu_{laser}$. The uncertainty of the term values thus obtained is determined by the line position accuracy and the additional systematic error caused by the uncertainty of the laser frequency within the generation contour; this uncertainty is the same for all lines belonging to the same progression.

III. ANALYSIS OF TERM VALUES

The total data set included in the current analysis of the $X^1\Sigma^+$ state term values was constructed of three parts. The first part contains the present measured 302 term values $T^{expt}_{v''J''}$ assigned to both $^{23}Na^{85}Rb$ and $^{23}Na^{87}Rb$ isotopomers corresponding to $v''\in[24,76]$; $J''\in[12,64]$ levels (see Table I). The second part contains 44 highly accurate (with a line position uncertainty $\sigma^{expt}_{v''J''}\approx 0.003\ cm^{-1}$) experimental term values for $v''\in[5,30]$; $J''=10,12$ levels of $^{23}Na^{85}Rb$ given in Table I of Ref. [12]. The third part contains eight $v''\in[0,3]$; $J''=10,12$ term values restored using the relevant G_v, B_v, D_v, and H_v molecular constants of the $^{23}Na^{85}Rb$ isotopomer given in Table I of Ref. [13]; it is assumed that the uncertainty of these data $\sigma^{expt}_{v''J''}$ does not exceed $0.003\ cm^{-1}$.

Altogether 354 term values of the NaRb $X^1\Sigma^+$ state were treated simultaneously by the combined-isotopomer weighted least-squares (WLS) fit,

$$\overline{\sigma}_f=\min\left[\frac{1}{N-M}\sum_{v''J''}^{N}\left(\frac{T^{expt}_{v''J''}-T^{calc}_{v''J''}}{\sigma^{expt}_{v''J''}}\right)^2\right]^{1/2}, \qquad (1)$$

where N is the total number of the experimental energies, and M is the number of the fitting parameters obtained below by both Dunham-type and direct potential fit analysis.

A. Dunham-type fit

Term values for the isotope-substituted NaRb molecule can be represented as a linear combination [20]

$$T^{\alpha}_{v''J''}=\sum_{(l,m)\neq(0,0)} Y_{l,m}X^{\alpha}_{l,m}+(1-\varepsilon^2_{\alpha})\sum_{(l,m)\geqslant(0,0)}\delta^{Rb}_{l,m}X^{\alpha}_{l,m} \qquad (2)$$

of the basis functions $X^{\alpha}_{l,m}$,

$$X^{\alpha}_{l,m}=\rho^{2m+l}_{\alpha}(v''+1/2)^l[J''(J''+1)]^m,$$

TABLE II. Dunham parameters (in cm^{-1}) for the $X^1\Sigma^+$ state of the $^{23}Na^{85}Rb$ isotopomer, obtained from a simultaneous fit (1, 2) to the total set of the experimental term values corresponding to both $^{23}Na^{85}Rb$ and $^{23}Na^{87}Rb$ isotopomers. The numbers in parentheses are equal to two standard deviations. Five additional fitting parameters corresponding to origin uncertainties in the present $C \rightarrow X$ LIF series are given in Table I. The value of Y_{00} is calculated.

$Y_{0,0}$	-0.0225	
$Y_{1,0}$	106.844973	$(\pm 7.3\times10^{-3})$
$Y_{2,0}$	-0.3769493	$(\pm 2.7\times10^{-3})$
$Y_{3,0}$	-1.3253577×10^{-3}	$(\pm 4.5\times10^{-4})$
$Y_{4,0}$	6.1584938×10^{-5}	$(\pm 4.1\times10^{-5})$
$Y_{5,0}$	-4.7069851×10^{-6}	$(\pm 2.2\times10^{-6})$
$Y_{6,0}$	1.8256265×10^{-7}	$(\pm 7.5\times10^{-8})$
$Y_{7,0}$	-4.4448825×10^{-9}	$(\pm 1.6\times10^{-9})$
$Y_{8,0}$	6.4873784×10^{-11}	$(\pm 1.9\times10^{-11})$
$Y_{9,0}$	-5.2293387×10^{-13}	$(\pm 1.3\times10^{-13})$
$Y_{10,0}$	1.7866377×10^{-15}	$(\pm 3.8\times10^{-16})$
$Y_{0,1}$	7.011329×10^{-02}	$(\pm 4.7\times10^{-5})$
$Y_{1,1}$	-2.823823×10^{-04}	$(\pm 3.8\times10^{-5})$
$Y_{2,1}$	1.558186×10^{-06}	$(\pm 6.2\times10^{-6})$
$Y_{3,1}$	-5.705886×10^{-07}	$(\pm 4.2\times10^{-7})$
$Y_{4,1}$	3.065820×10^{-08}	$(\pm 1.5\times10^{-8})$
$Y_{5,1}$	-7.845547×10^{-10}	$(\pm 2.8\times10^{-10})$
$Y_{6,1}$	9.305117×10^{-12}	$(\pm 2.7\times10^{-12})$
$Y_{7,1}$	-4.254388×10^{-14}	$(\pm 1.0\times10^{-14})$
$Y_{0,2}$ [a]	-1.2107×10^{-7}	$(\pm 4.0\times10^{-11})$
$Y_{1,2}$ [a]	-9.50×10^{-10}	$(\pm 2.4\times10^{-11})$
$Y_{2,2}$	1.78×10^{-10}	$(\pm 1.9\times10^{-10})$
$Y_{3,2}$	-1.92×10^{-11}	$(\pm 1.1\times10^{-11})$
$Y_{4,2}$	5.3×10^{-13}	$(\pm 2.1\times10^{-13})$
$Y_{5,2}$	-4.6×10^{-15}	$(\pm 1.3\times10^{-16})$
$Y_{0,3}$ [a]	2.08×10^{-13}	$(\pm 1.0\times10^{-15})$
No. of data	354	
Total no. of parameters	31	
No. of fitting parameters	27	
$\overline{\sigma_f}$	1.18	

[a]Value and uncertainty are taken from Table III of Ref. [13].

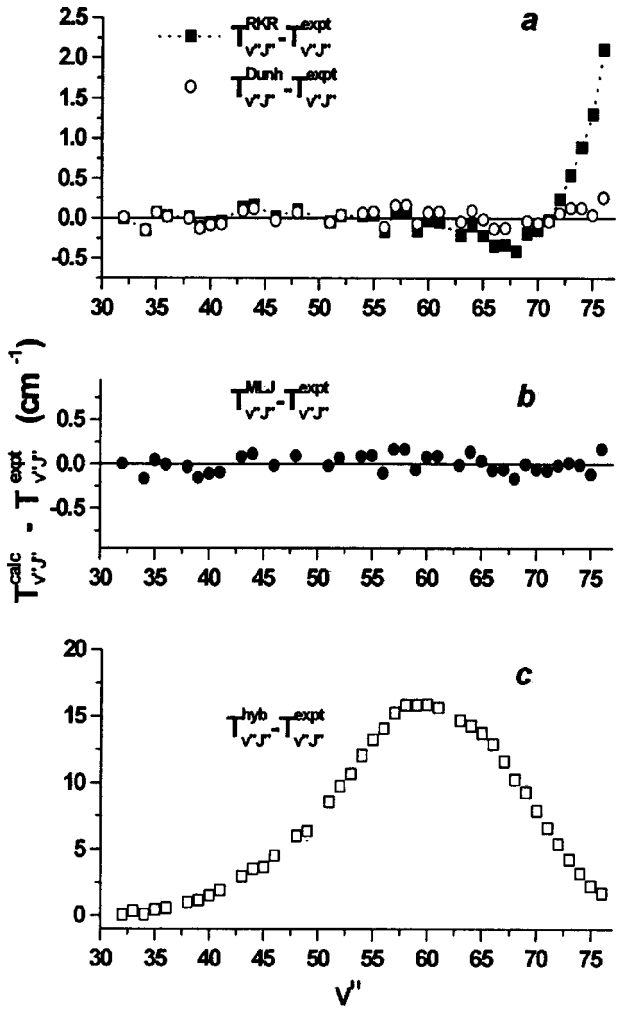

FIG. 3. Differences between calculated $T^{calc}_{v''J''}$ and experimental $T^{expt}_{v''J''}$ term values for $^{23}Na^{85}Rb$ $X^1\Sigma^+(v''>30, J''=25)$. (a) $T^{Dunh}_{v''J''}$ are calculated by Dunham constants from Table II and $T^{RKR}_{v''J''}$ by the present RKR; (b) $T^{MLJ}_{v''J''}$ are calculated by the present direct MLJ potential fit analysis; (c) $T^{hyb}_{v''J''}$ are calculated by the preceding hybrid potential [14].

where $Y_{l,m}$ are the required Dunham coefficients [8] while $\delta^{Rb}_{l,m}$ are the modified in Ref. [20] Born-Oppenheimer (BO) and JWKB breakdown parameters [21–23]. The reduced mass ratio parameters for the $^{23}Na^{87}Rb$ pattern are $\rho_\alpha = \sqrt{\mu_{^{23}Na^{85}Rb}/\mu_{^{23}Na^{87}Rb}}$ and $\varepsilon_\alpha = \sqrt{M_{^{85}Rb}/M_{^{87}Rb}}$, while $\rho_\alpha = \varepsilon_\alpha = 1$ for the most abundant $^{23}Na^{85}Rb$ isotopomer, μ is the reduced molecular mass and M is the respective atomic mass of the Rb isotope.

The Dunham parameters $Y_{l,m}$ of the $^{23}Na^{85}Rb$ isotopomer presented in Table II were obtained by the weighted linear LS fitting procedure (1) accompanied by experimental determination of the optimum power degrees (l_{max}, m_{max}) for each vibrational and rotational expansion in Eq. (2). During the fit the lowest centrifugal distortion constants (CDCs) $Y_{0,2}$, $Y_{1,2}$, and $Y_{0,3}$ were held fixed at the values obtained from highly accurate $v'' \in [0,6]$; $J'' \in [0,80]$ term energies, see Table III in Ref. [13]. Five adjustable parameters $\Delta T^{Dunh}_{v'J'}$ presented in Table I were added to the fitting procedure to remove systematic errors caused by an uncertainty of the present experimental series origin, i.e., $T^{expt}_{v'J'}$. In the framework of the Dunham-type analysis a correctness of the term values assignment given above was additionally tested by a trial-and-error method, i.e. the isotopic assignment and/or rotational numbering were consequently variated for each P,R pair of the particular LIF progression. The sharp global minimum of the functional (1) was observed with the assignment given in Table I. BO breakdown effects have not been observed since no parameter $\delta^{Rb}_{l,m}$ was found to be required to approximate the present combined-isotopomer data within their experimental uncertainties. The resulting molecular constants presented in Table II reproduce the high accuracy data [12,13] corresponding to $J''=10,12$ levels with rms $=0.002$ cm^{-1} while the present experimental term values are reproduced with rms $=0.1$ cm^{-1}. The $Y_{0,0}$ value in Table II was evaluated by the Dunham relation [8].

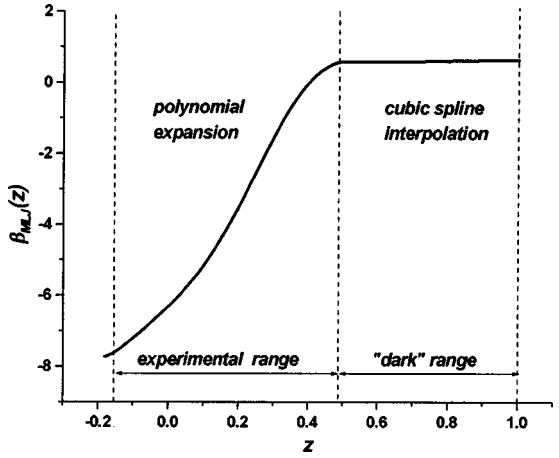

FIG. 4. Smooth polynomial plus cubic spline approximation of the exponent parameter $\beta(z)$ for the MLJ potential (4) of the NaRb ground state.

The Birge-Sponer (BS) extrapolation of the last $\Delta G(v'')$ values $G(v'')=\Sigma_{l=1}^{l_{max}} Y_{l,0}(v''+1/2)^l$ together with extrapolation of the $B(v'')=\Sigma_{l=0}^{l_{max}} Y_{l,1}(v''+1/2)^l$ function to a dissociation limit predicts the last bound level $v_D''=79$ and the dissociation energy $D_e=5032\pm 2$ cm^{-1}. These estimates are rather close to their more accurate counterparts $v_D''=81$ and $D_e=5030.75\pm 0.1$ cm^{-1} obtained by the hybrid potential [14], as well as to $D_e=5030\pm 2$ cm^{-1} value obtained by the BS extrapolation of the $a^3\Sigma^+$ state molecular constants [13].

The resulting $G(v'')$ and $B(v'')$ expansions were further applied to a conventional first-order RKR potential construction [24] up to the last observed vibrational level $v''=76$. A nonphysical bend (a ''turning over'') had appeared in the inner wall of the RKR curve for $v''\geqslant 55$ levels. This means that the obtained vibrational and rotational constants are not self-consistent for upper vibrational levels due to strong correlation between the rotational and CDC parameters. The bend problem was solved by the exponential extrapolation $U_{in}(R)\equiv G(v''=54)\times e^{-b(R-R_-(v''=54))}$, where parameter b was obtained by matching smoothly the slope of the RKR potential at the left-turning point $R_-(v''=54)$. The corrected left-turning points for the upper levels were then found by a solution of the equation $U_{in}(R_-^{shift})=G(v''\geqslant 55)$, while the associated right-turning points were determined as $R_+^{shift}(v'')=R_-^{shift}(v'')+\Delta R(v'')$. The required $\Delta R(v'')=R_+(v'')-R_-(v'')$ values were estimated using the RKR $f(v'')$ integrals, which are dependent on vibrational constants only [24].

The derived RKR potential as well as the existing hybrid potential [14] were used to evaluate the term values $T_{v''J''}^{RKR}$ and $T_{v''J''}^{hyb}$ by a numerical solution of the radial Schrödinger equation, see below. The obtained $T_{v''J''}^{RKR}$ values agree better with both preceding [12,13] ($\mathrm{rms}_{RKR}=0.007$ cm^{-1}) and present ($\mathrm{rms}_{RKR}=0.3$ cm^{-1}) experimental data than their $T_{v''J''}^{hyb}$ counterparts ($\mathrm{rms}_{hyb}=0.018$ and 6.4 cm^{-1}, respectively). The quality of Dunham, RKR, and hybrid approaches is illustrated by Figs. 3(a) and 3(c). In contrast to $T_{v''J''}^{Dunh}$ and $T_{v''J''}^{RKR}$ term values, the $T_{v''J''}^{hyb}$ ones systematically deviate from the experimental data for $v''>35$, the difference reaching its maximum at $v''\simeq 58$. At the same time, the pronounced systematic errors of the $T_{v''J''}^{RKR}$ values corresponding to highest vibrational terms still remain, see Fig. 3(a). The situation could probably be improved by employing an iterative self-consistent procedure [25–27] based on constrained Dunham-fit with the improved CDC values calculated by the initial RKR potential [28]. However, such procedure seems to be not feasible due to limited accuracy and volume of present experimental data related to high rotational levels.

TABLE III. MLJ potential (4) parameters for the $X^1\Sigma^+$ state of NaRb obtained from a direct fit to total bulk of the experimental term values corresponding to both ^{23}Na^{85}Rb and ^{23}Na^{87}Rb isotopomers. The numbers in parentheses are equal to two standard deviations. Five additional fitting parameters corresponding to the origin uncertainties in the present $C\rightarrow X$ LIF series are given in Table I.

D_e (cm^{-1})	5030.75 [a]	(± 0.10) [a]
R_e (Å)	3.64421	($\pm 1.1\times 10^{-3}$)
β_0	-6.312091	($\pm 4.4\times 10^{-4}$)
β_1	9.665262	($\pm 7.1\times 10^{-4}$)
β_2	12.70902	($\pm 1.2\times 10^{-3}$)
β_3	65.58015	($\pm 2.3\times 10^{-3}$)
β_4	-15.30441	($\pm 4.3\times 10^{-3}$)
β_5	-643.6652	($\pm 3.1\times 10^{-2}$)
β_6	2488.876	(± 0.30)
β_7	-10772.84	(± 0.78)
β_8	22720.46	(± 0.74)
β_9	-16240.38	(± 0.46)
R_M (Å)	11.0	
b_∞	0.638804	
b_2	-0.986641	
b_3	-1.525996	
No. of data	354	
Total No. of parameters	21	
No. of fitting parameters	16	
$\overline{\sigma_f}$	1.27	

[a]Value and uncertainty are borrowed from Ref. [14].

B. Direct modified Lennard-Jones potential fit

Recently the DPF analysis has proved [10,11] to be a more compact and more physically justified method to approximate high vibrational and rotational term values of adiabatic diatomic states corresponding to different isotopomers than the conventional Dunham fit accompanied by the relevant RKR potential construction. In the framework of the DPF approach the required adiabatic potentials $U^\alpha(R)$ are obtained by the weighted nonlinear least-squares (WNLS) fitting procedure (1), where the calculated rovibronic term values $T_{v''J''}^{calc}\equiv T_{v''J''}^{\alpha}$ are the eigenvalues of the uncoupled radial Schrödinger equation (in atomic units):

TABLE IV. Experimental term values T^{expt} of the $^{23}Na^{87}Rb$ quasibound levels and their theoretical counterparts T^{calc} obtained from the present MLJ potential. T_{BS}^{calc} were evaluated by the Bohr-Sommerfeld rule [33], while T_{ST}^{calc} with the respective widths Γ_{ST}^{calc} were estimated using the ''stabilization'' method [32]. All values are in cm^{-1}. Numbers in parentheses are equal to two standard deviations. T^{expt} are corrected for the origin shift according to the last column of Table I.

v''	J''	T^{expt}	T_{BS}^{calc}	T_{ST}^{calc}	Γ_{ST}^{calc}
70	59	5038.44 ($\pm$ 0.24)	5038.62	5038.62	<0.01
71 [a]	59	5045.29 ($\pm$0.24)	5045.42	5045.41	<0.01
72 [b]	59		5048.06	5048.61	0.92
69	61	5033.61 ($\pm$0.26)	5033.67	5033.67	<0.01
70	61	5042.61 ($\pm$0.28)	5042.70	5042.67	<0.01
71 [b]	61		5048.71	5048.66	<0.01
69	62	5036.12 ($\pm$0.18)	5036.04	5036.04	<0.01
70	62	5044.58 ($\pm$0.18)	5044.74	5044.73	<0.01
71 [a]	62	5050.14 ($\pm$0.16)	5050.28	5050.19	0.08
69	64	5040.75 ($\pm$0.18)	5040.78	5040.77	<0.01
70	64	5048.70 ($\pm$0.18)	5048.76	5048.75	<0.01
71 [a]	64	5052.84 ($\pm$0.24)	5053.06	5052.72	0.71

[a]Levels are omitted from the MLJ fitting procedure.
[b]Levels correspond to overlapped lines.

$$\left(-\frac{d^2}{2\mu_\alpha dR^2} + U^\alpha(R) + \frac{J''(J''+1)}{2\mu_\alpha R^2} - T^\alpha_{v''J''} \right) \chi^\alpha_{v''J''}(R) = 0. \tag{3}$$

Here $\chi^\alpha_{v''J''}$ are the adiabatic rovibronic eigenfunctions. Since the reduced masses μ_α of the $^{23}Na^{85}Rb$ and $^{23}Na^{87}Rb$ isotopomers are very close to each other, the difference in the respective adiabatic correction to the relevant Born-Oppenheimer potential can be neglected. Hence, the adiabatic potentials for both isotopomers can be represented by a single mass-independent curve $U^\alpha = U^{85} = U^{87}$. In the present work the analytical ''modified Lennard-Jones'' potential [11] was applied,

$$U_{MLJ}(R) = D_e[1 - (R_e/R)^n e^{-\beta(z)z}]^2, \tag{4}$$

where D_e is the dissociation energy, R_e is the equilibrium bond length and $z(R;p=1) = (R^p - R_e^p)/(R^p + R_e^p)$ is the dimensionless generalized variable [29]. The power $n=6$ predicts correct long-range behavior of the NaRb ground-state potential $U(R) \sim D_e - C_6/R^6$ dissociated into two ^1S state atoms [15].

In the z region covered by the experimental term values the exponent parameter $\beta(z)$ is approximated by the ordinary polynomial expansion $\Sigma_{m=0}^M \beta_m z^m$. To extrapolate the $\beta(z)$ function to the ''dark'' interval between the region covered by experimental data and the dissociation limit, the ordinary cubic spline $\beta_E(z) = \Sigma_{n=0}^3 b_n (z-1)^n$ was adopted, see Fig. 4. Respective coefficients $b_0 = \beta_\infty$, $b_1 = 0$, $b_2 = [3(\beta_M - b_0) - \beta'_M(z_M - 1)]/(z_M - 1)^2$, and $b_3 = [\beta'_M - 2b_2(z_M - 1)]/3(z_M - 1)^2$ are determined by matching smoothly the $\beta(z)$ polynomial expansion at the meeting point $z_M = (R_M - R_e)/(R_M + R_e)$ ($\beta_M \equiv \beta_E(z_M) = \beta(z_M)$; $\beta'_M \equiv \partial\beta_E(z_M)/\partial z = \partial\beta(z_M)/\partial z$) and the boundary conditions at $R \to \infty$, i.e. $\beta_E(1) = \beta_\infty$ and $\partial\beta_E(1)/\partial z = 0$.

The $\beta_\infty = 0.638$ value was estimated according to $\beta_\infty = \ln[2D_e(R_e)^6/C_6]$ [11], where the dispersion coefficient C_6 was taken from Ref. [15]. The matching point $R_M = 11$ Å was fixed at near the right-turning point of the last-observed vibrational level $v'' = 76$. The equilibrium distance R_e, polynomial coefficients β_m ($m \in [0,9]$), as well as the origins of the present five LIF series were considered as adjustable fitting parameters during the WNLS fit. The required initial set of the R_e and β_m values was estimated by a transformation of the present RKR potential to its MLJ counterpart. The $D_e = 5030.75$ cm^{-1} value [14] was fixed during the fit as considering dissociation energy as a free parameter in the MLJ approach has often been found to yield a D_e value underestimated by a number of wave numbers [10]. The minimum of the functional (1) was searched by a modified Levenberg-Marquardt algorithm combined with a finite-difference approximation of the corresponding Jacobian matrix [30]. The resulting MLJ potential given in Table III reproduces low J-term values from Refs. [12,13] with rms $= 0.004$ cm^{-1} while the present experimental term values with rms $= 0.1$ cm^{-1}.

Since quasibound rovibronic levels seem to be very sensitive to the behavior of the rotationless potential $U^\alpha(R)$ near dissociation limit, the experimental term values belonging to the $^{23}Na^{87}Rb$ isotopomer and lying above $D_e = 5030.75$ cm^{-1} (except the last vibrational levels which are strongly predissociated) were also incorporated into the MLJ potential fit. To confirm the reliability of the derived potential, the resonance energies and widths of the last quasibound levels $v'' = 71$ and 72 were predicted and compared with the available experimental results, see Table IV.

C. Computational details

For all bound and quasibound rovibronic levels under consideration the radial equation (3) was solved numerically by a finite difference (FD) method [31]. The rovibronic wave functions, as well as adiabatic and centrifugal distortion potentials were tabulated at N equally spaced intervals $h = R_i - R_{i-1}$, while the second derivative d^2/dR^2 was replaced by the five-point central difference at each tabulated position. A solution of the derived N simultaneous FD equations was then reduced to the eigenvalues search of the real symmetric five-bands matrice [30]. To improve the accuracy of derived eigenvalues, the FD equations were solved for two stepsizes h_1, $h_2 = 2h_1$, and the eigenvalues were extrapolated to $h \to 0$ assuming h^4 dependence of the discretization error, i.e. $T^{calc}_{v''J''} = T^{calc}_{h_1} + \delta^{calc}$, where $\delta^{calc} = [T^{calc}_{h_2} - T^{calc}_{h_1}]/15$. Satisfactory convergence ($\delta^{calc} < \sigma^{exp}$) of the integration was achieved with $h_1 = 0.001$ Å for the internuclear distance $R \in [2.4, R_M]$ Å , where the right boundary point R_M was variated in the interval $R_M \in [15,25]$ Å. Both resonance energies and widths of the quasibound levels were calculated by a stabilization method [32] from the change in the $T^{calc}_{v''J''}(R_M)$ function as the R_M value increases. The simple Bohr-Sommerfeld quantization rule [33] was also applied to evaluate both bound and quasibound term values. As was expected, the semiclassical estimates were remarkably close (within 0.02 cm^{-1} value corresponding to the second-order JWKB correction given by the Dunham parameter $|Y_{0,0}| = 0.023$ cm^{-1}) to their quantum counterparts, see Table IV, with the exception of the last quasibound levels lying near the top of the centrifugal distortion barrier.

IV. CONCLUDING REMARKS

The analytical MLJ construction allowed us to match gently the previous highly accurate experimental term values available for the bottom of the potential with its long-range behavior through the intermediate v'' region completely covered by present measurements. In spite of the moderate accuracy of the current measurements the derived adiabatic MLJ potential for the NaRb $X^1\Sigma^+$ ground state in the $v'' \gtrsim 35$ region, appears to be more accurate than the preceding hybrid potential [14]. However, highly accurate experimental term values for the extended range of rotational levels would be desirable for significant improvement of the ground-state potential.

ACKNOWLEDGMENTS

The authors are indebted to Professor William C. Stwalley for numerous fruitful discussions. Professor Robert J. LeRoy is especially thanked for a critical reading of the manuscript and helpful suggestions. The Moscow team acknowledges the financial support of the Russian Foundation of Basic Research under Grant No. 00-03-32978. The Riga team acknowledges the financial support of the Latvian Science Council under Grant No. 01.0264. Both groups acknowledge the NATO Science Program Cooperative Linkage Grant No. 977428.

[1] H. Wang and W.C. Stwalley, J. Chem. Phys. **108**, 5767 (1998).
[2] A. Zaitsevskii, S.O. Adamson, E.A. Pazyuk, A.V. Stolyarov, O. Nikolayeva, O. Docenko, I. Klincare, M. Auzinsh, M. Tamanis, R. Ferber, R. Cimiraglia, Phys. Rev. A **63**, 052504 (2001).
[3] M. Tamanis, R. Ferber, E. A. Pazyuk, A. V. Stolyarov, A. V. Zaitsevskii, H. Chen, J. Qi, H. Wang, and W. C. Stwalley, J. Chem. Phys. **117**, 7980 (2002).
[4] A.J. Ross, C. Effantin, J. d'Incan, and R.F. Barrow, Mol. Phys. **56**, 903 (1985).
[5] W.T. Zemke and W.C. Stwalley, J. Chem. Phys. **111**, 4956 (1999).
[6] C. Amiot and J. Verges, J. Chem. Phys. **112**, 7068 (2000).
[7] F. Martin, P. Crozet, A.J. Ross, M. Aubert-Frecon, P. Kowalczyk, W. Jastrzebski, and A. Pashov, J. Chem. Phys. **115**, 4118 (2001).
[8] J.L. Dunham, Phys. Rev. **41**, 713 (1932); *ibid.* **41**, 721 (1932).
[9] W.M. Kosman and J. Hinze, J. Mol. Spectrosc. **56**, 93 (1975); C.R. Vidal and H. Scheingraber, *ibid.* **65**, 46 (1977).
[10] J.Y. Seto, R.J. Le Roy, J. Verges, and C. Amiot, J. Chem. Phys. **113**, 3067 (2000).
[11] P.G. Hajigeorgiou and R.J. Le Roy, J. Chem. Phys. **112**, 3949 (2000).
[12] S. Kasahara, T. Ebi, M. Tanimura, H. Ikoma, K. Matsubara, M. Baba, and H. Katô, J. Chem. Phys. **105**, 1341 (1996).
[13] Y.-C. Wang, M. Kajitani, S. Kasahara, M. Baba, K. Ishikawa, and H. Katô, J. Chem. Phys. **95**, 6229 (1991).
[14] W.T. Zemke and W.C. Stwalley, J. Chem. Phys. **114**, 10811 (2001).
[15] M. Marinescu and H.R. Sadeghpour, Phys. Rev. A **59**, 390 (1999).
[16] M.I. Chibisov and R.K. Janev, Phys. Rep. **166**, 1 (1988).
[17] M. Korek, A.R. Allouche, M. Kobeissi, A. Chaalan, M. Dagher, K. Fakherddin, and M. Aubert-Frecon, Chem. Phys. **256**, 1 (2000).
[18] N. Takahashi and H. Katô, J. Chem. Phys. **75**, 4350 (1981).
[19] O. Nikolayeva, I. Klincare, M. Auzinsh, M. Tamanis, R. Ferber, E.A. Pazyuk, A.V. Stolyarov, A. Zaitsevskii, and R. Cimiraglia, J. Chem. Phys. **113**, 4896 (2000).
[20] R.J. Le Roy, J. Mol. Spectrosc. **194**, 189 (1999).
[21] A.H.M. Ross, R.S. Eng, and H. Kildal, Opt. Commun. **12**, 433 (1974).
[22] P.R. Bunker, J. Mol. Spectrosc. **68**, 367 (1977).
[23] J.K.G. Watson, J. Mol. Spectrosc. **80**, 411 (1980).
[24] R. Rydberg, Z. Phys. **73**, 376 (1931); O. Klein, *ibid.* **76**, 226 (1932); A.L.G. Rees, Proc. Phys. Soc. London **59**, 998 (1947).
[25] R.J. LeRoy and R.B. Bernstein, J. Chem. Phys. **52**, 3869 (1970).
[26] R. J. Le Roy, *Specialist Periodical Reports, Molecular Spectroscopy* (Chemical Society, London, 1973), Vol. 1, p. 113.
[27] J.D. Brown, G. Burns, and R.J. LeRoy, Can. J. Phys. **51**, 1664 (1973).
[28] J.M. Hutson, S. Gerstenkorn, P. Luc, and J. Sinzelle, J. Mol. Spectrosc. **96**, 266 (1982).

[29] A.A. Surkus, R.J. Rakauskas, and A.B. Bolotin, Chem. Phys. Lett. **105**, 291 (1984).
[30] W. H. Press, S. A. Teukolsky, W. T. Vetterling, and B. P. Flannery, *Numerical Recipes in Fortran 77* (Cambridge University Press, Cambridge, 1999).
[31] K.P. Lawley, J. Comput. Phys. **70**, 218 (1987).
[32] A.U. Hazi and H.S. Taylor, Phys. Rev. A **1**, 1109 (1970).
[33] L. D. Landau and E. M. Lifshits, *Quantum Mechanics* (Pergamon Press, New York, 1965).